Polymer 51 (2010) 4340–4350

Contents lists available at ScienceDirect

Polymer

journal homepage: www.elsevier.com/locate/polymer

Reactive blending as a tool for obtaining poly(ethylene terephthalate)-based engineering materials with tailored properties

Siyamak Safapour [a], Mirhadi Seyed-Esfahani [a,**], Finizia Auriemma [b,*], Odda Ruiz de Ballesteros [b], Paolo Vollaro [b], Rocco Di Girolamo [b], Claudio De Rosa [b], Ali Khosroshahi [a]

[a] Department of Textile Engineering, Amirkabir University of Technology, Hafez Avenue, P.O. Box 15875-4413, Tehran, Iran
[b] Dipartimento di Chimica "Paolo Corradini", Università di Napoli "Federico II", Complesso Monte S.Angelo, Via Cintia, I-80126 Napoli, Italy

ARTICLE INFO

Article history:
Received 18 May 2010
Accepted 8 July 2010
Available online 4 August 2010

Keywords:
Reactive blending
Engineering materials
Diffraction analysis

ABSTRACT

The structure and properties of blends of poly(ethylene terephthalate) (PET) with poly(trimethylene terephthalate) (PTT) at PTT concentration ≤30 wt.%, obtained with three different methods: from solution, melt extrusion, and direct spinning, are investigated. Relationships between the method of preparation and properties of blends are established. All blends show glass transition temperature at values determined by composition, and crystallization properties also dependent on the preparation method. Blends obtained from solution show separated melting of components. For blends obtained from the melt only PET crystallizes. The melting temperature decreases with the residence time of the melt at high temperatures, due to occurrence of ester exchange reactions. It is shown that reactive blending of PET/PTT mixtures occurring during preparation is a versatile route for obtainment of engineering materials with good mechanical properties, high crystallinity, glass transition temperature lower than that of PET, and melting temperature that may be controlled by the processing conditions.

1. Introduction

Poly(ethylene terephthalate) (PET), poly(trimethylene terephthalate) (PTT), and poly (butylene terephthalate) (PBT) are thermoplastic engineering materials of large commercial importance, thanks to their outstanding physical and mechanical properties such as high strength, stiffness, toughness and heat resistance [1]. PET is the highest-volume polyester produced and is used in numerous applications such as films, fibers, and packaging [1,2]. PBT is namely used as an insulator in the electrical and electronics industries. Compared to PET, PBT has lower strength and rigidity, better impact resistance, and a lower glass transition temperature [1,2]. PTT is the youngest member of the series to reach industrial production because of the relatively high price of 1,3-propenediol monomer. Only after development of a low cost innovative synthetic process for production of 1,3-propenediol based on hydroformilation of ethylene oxide using a soluble catalyst in 1995 [3], the Shell Chemicals started PTT mass production. In PTT the properties of PET of high performance plastomer are combined with those of PBT showing better processing characteristics, better elastic recovery and higher crystallization rate than PET. PTT, indeed, can be easily spun into fibers and yarns, and can be used in numerous applications such as carpeting, textiles and apparel, engineering thermoplastics, nonwovens, films and monofilaments [4–7].

The introduction of PTT into the market has greatly enhanced the research interest for this polymer also because of the possibility of obtaining binary blends of PTT with other polyesters, in particular with PET, showing combined useful properties of both components. Blending, indeed, is a simple, economical, and versatile route to produce new materials with tailored properties, without resorting to the synthesis of a totally new compound [8].

Binary blends of PET and PTT have been recently studied. It has been shown that the two components are completely miscible in the glassy state in the whole composition range, independent of preparation method, i.e. solution blending and melt-blending [9–12]. A single glass transition temperature is indeed observed, gradually decreasing with PTT content from the value of pure PET (≈89 °C) to that of pure PTT (≈35 °C). In the case of blends prepared by co-precipitation of the two components from solution, it has been shown that as precipitated samples show independent melting of the two components at temperatures close to the melting temperature of neat PET and PTT [12]. The two polyesters do not form co-crystals [9–12], even though, for short residence

* Corresponding author. Tel.: +39 081 674341; fax: +39 081 674090.
** Corresponding author. Tel.: +98 21 64542618; fax: +98 21 66400245.
E-mail addresses: esfahani@aut.ac.ir (M. Seyed-Esfahani), finizia.auriemma@unina.it (F. Auriemma).

0032-3861/$ – see front matter © 2010 Elsevier Ltd. All rights reserved.
doi:10.1016/j.polymer.2010.07.011

time of the melt at high temperature, they crystallize simultaneously, with formation of crystals within the same spherulites [9]. For blends obtained by melt processing of the two components, or by prolonged heat treatment of solution blends at high temperatures in the melt state, ester exchange reactions between the chains of the two components occur, leading to formation of copolymer chains with the potential to act as compatibilizer [9–12]. The extent to which transesterification reactions occur depends on the initial degree of compatibility, and on blending parameters such as maximum temperature achieved in the melt, duration of heat treatment and mixing parameters, viscosity match, etc. [9–12]. The most remarkable effect of transesterification reactions is in the emergence of a single melting temperature of the blends with a tendency of the melting endotherm to move toward lower temperatures with the residence time of the melt at high temperatures [9,12].

With the aim to exploit the lower glass transition temperature of PET/PTT blends and/or the intrinsic elastic properties of PTT fibers without impairing the good mechanical performance of PET, the possibility of production of fibers by blending PET with PTT has been also explored. It has been shown [13] that for fibers containing 10 wt.% PTT, an improvement of elastic recovery without drop of tenacity and modulus in comparison to pure PET fibers is achieved, and that the dyeing ability for PTT content of ≈30 wt.% is superior to that of PET and even better than that of pure PTT fibers. Therefore, the studies performed to date indicate that PTT is an excellent candidate for obtainment of PET-based materials with properties intermediate between those of the two components, or even with better performance.

In the studies performed to date a direct relationship between the effect of reactive blending on the structure, physical and mechanical properties of PET/PTT blends obtained via different methods has not been yet performed. In this paper a detailed structural investigation is performed on PET rich blends with PTT aimed at establishing direct relationships between the method of preparation of the blends, their structure, thermal and physical properties. To this aim, PET/PTT blends in the composition range 5–30 wt.% of PTT have been prepared according to three different methods, i.e. by precipitation from solution (solution blends, SB) melt extrusion (MB) and direct melt spinning of mechanical mixtures of the two components to obtain fibers (FB). The use of the direct spinning method for the preparation of blend fibers relies on the miscibility of PET and PTT in the melt state without any need of adding a third component as compatibilizer. It allows obtaining fibers from the two polyesters without the need to prepare blend chips prior spinning, as a necessary step generally used to achieve an effective dispersion of the components [8,14].

The structure and properties of all blends are analyzed and compared also with those of samples of the pure components prepared following the same procedure. This is the first comparative and systematic investigation of the effect of the preparation method on the structure and properties of PET/PTT blends. This study is aimed not only at clarifying basic aspects related to the unavoidable occurrence of reactive blending of PET and PTT chains during the preparation step and successive heat treatments, but also to highlight the beneficial effect of ester exchange reactions on the final properties of this class of new materials, especially suited for applications in fiber technology.

2. Experimental section

2.1. Materials

PET and PTT chips used in this study are commercial grades from Tondgooyan petrochemical company, Iran, and Shell chemical company, USA, respectively. Shapes of PET and PTT chips are cylindrical and spherical with approximate number of chips per gram of 36–40 and 39–44, respectively. Solvents of analytical grade have been purchased from Aldrich and used as received. The commercial grade of PET sample contains 0.34 wt.% TiO_2 as de-lustering agent [15a] and corresponds to 1.01 wt.% diethylene glycol content [15b] and 21 meq/kg carboxyl end groups concentration [15c]. Intrinsic viscosity (IV) has been measured at 25 °C for PET and 30 °C for PTT using an Ubbelohde viscometer in a 60/40 wt.% mixture of phenol/1,1,2,2 tetrachloroethane [16] For PET and PTT, intrinsic viscosity values of 0.65 and 0.92 dL/g have been calculated, respectively. For PET, the number average molecular mass M_n of 24 kDa has been obtained from the intrinsic viscosity value using the relationship $[\eta] = K\ M_n^{\alpha}$, with $K = 7.61\ 10^{-4}$ and $\alpha = 0.67$ for PET [16a], whereas for PTT the relationship $[\eta] = K'\ M_w^{\alpha}$ with $K' = 5.36\ 10^{-4}$ and $\alpha = 0.69$ has been used, giving a mass average molecular mass M_w of 48 kDa ($M_w/M_n \approx 2$ in both cases) [16b].

2.2. Preparation of blends

Chips of the two polyesters have been first dried in a vacuum oven at 140 °C for 24 h prior their usage. Successively, weighted amounts of the dried samples have been mechanically mixed to obtain PET/PTT mixtures at weight percent ratio 95/5, 90/10, 80/20 and 70/30 to be used for the preparation of blends. Three different methods have been used to prepare the samples: precipitation from solution, extrusion from the melt and direct spinning of mechanical mixtures of the components from the melt to obtain fibers. The direct spinning of the mixtures of the two components from the melt implies that no additional step for the preparation of blend chips is used to obtain the fibers. Pure PET and pure PTT samples have been also obtained using the same procedures of the blends, in order to have a more direct comparison of the properties of the blends with those of pure components. Here in the following the samples obtained according to three different methods will be indicated with symbols SB for the systems obtained from solution, MB for those obtained by melt extrusion and FB for the fibers.

2.2.1. Solution blends

Pure components as well as their mechanical mixtures have been dissolved at 60 °C in chloroform/trifluoroacetic 80/20 v/v solutions, precipitated by addition of methanol and then dried in a vacuum oven at 80 °C for 24 h.

2.2.2. Melt extruded blends

Melt extrusion has been conducted under nitrogen atmosphere using a single-screw extruder ($L/D = 25$, $D = 35$ mm with L and D the length and diameter of screw) equipped with static mixer and a die section. Four different zone temperatures of 250, 270, 280, and 290 °C (230, 240, 250 and 260 °C for pure PTT) have been used corresponding to the feeding, metering, melt-blending, and die units, respectively for a total residence time of the melt in the extruder of ≈15 min.

2.2.3. Preparation of fibers

Melt spinning has been conducted in nitrogen atmosphere using the same screw extruder apparatus as before, but coupled to a spinneret unit having 36 circular holes, each of 0.25 mm diameter. Five different zone temperatures of 250, 270, 280, 290, and 290 °C have been employed corresponding to the feeding, metering, melt-blending, die, and spinneret block, respectively. For pure PTT the five temperature zone were at 230, 240, 250, 260 and 260 °C. Also in this case the processing conditions have been controlled in such a way that the total residence time of the melt in the spinning

extruder was ≈15 min. Partially Oriented Yarns (FB-POY) have been prepared at the take-up speed of 3500 m/min with a good constant spinning ability regardless of composition. Fully Drawn Yarns (FB-FDY) have been also produced by drawing the FB-POY samples using a drawing machine at speed of 400 m/min and drawing temperature of 90 °C for pure PET and blends, and 60 °C for PTT. The plate heater temperature has been fixed equal to 180 °C for the blends and PET, 150 °C for PTT. The drawing conditions for obtainment of FDY have been set up to reach draw ratios (D.R.) values nearly coinciding with 80% of the maximum elongation achieved by corresponding POY samples before breaking. The so fixed D.R. values are 1.39, 1.40, 1.43, 1.45, 1.55 and 1.34 for pure PET, 95/5, 90/10 80/20, 70/30 blends and pure PTT, respectively.

2.3. Differential scanning calorimetry (DSC)

DSC measurements have been performed under nitrogen atmosphere using a Mettler-DSC822/2285 apparatus Differential Scanning Calorimeter. Indium has been used as a calibration standard. The weight of the samples has been kept between 6 and 8 mg, and the scanning rate of 10 °C/min has been employed for all tests. The degree of crystallinity has been evaluated by the ratio of experimental values of melting enthalpy ΔH_m measured in DSC scans and the melting enthalpy of 100% crystalline polyesters ΔH_m° of 125 J/g for PET [17a] and 146 J/g for PTT [17b].

2.4. X-ray diffraction

X-ray powder diffraction profiles have been obtained with Ni filtered Cu Kα radiation using an automatic Philips diffractometer.

X-ray diffraction patterns of fibers have been recorded using a single crystal KCCD Nonius automatic diffractometer, (MoKα radiation, graphite single crystal monochromator), provided with an area detector for collection of bi-dimensional images and adapted for precise measurements of diffraction intensity distribution from fibers. For each sample, at least five consecutive bi-dimensional patterns have been recorded using 372 s exposition time/pattern, which have been then summed up using the program FIT2D available free of charge at WEB site http://www.esrf.eu/computing/scientific/FIT2D/ [18], to obtain X-ray fiber diffraction photographs with improved signal to noise ratio of 31 min total exposure time.

2.5. Mechanical tests

Tenacity-strain curves of fibers have been measured using a universal testing machine Zwicky by Zwick Roell. For each sample, after conditioning for 24 h at 25 °C and 65% relative humidity, multifilament yarns 100 mm in length have been examined at a crosshead speed of 500 mm/min with a preload of 0.5 cN/tex. We recall that tex is the unit of measurement of linear density used for fiber yarns and 1 tex corresponds to 10^{-6} Kg/m. Tenacity corresponds to the ratio of applied load and linear density. Mechanical parameters have been obtained by averaging the results measured for at least 10 independent specimens. The initial modulus has been calculated from the stress at 0.5–1% deformation in the stress-strain curve.

2.6. Solution ^{13}C NMR analysis

Solution ^{13}C NMR spectra of PET/PTT blends have been recorded at 25 °C with a Bruker Avance400 NMR spectrometer operating at 400.03 MHz, using tetramethylsilane as standard. The samples were dissolved in a mixed solvent of deuterated trifluoroactic acid and chloroform (1:3 volume ratio). A 90° pulse with ZGDC standard pulse sequence (with NOE and decoupling) was applied with delay time between consecutive FID acquisitions of 5 s.

3. Results and discussions

3.1. Thermal analysis

DSC thermograms of blends have been recorded during first heating, successive cooling and second heating scans in the case of as precipitated SB and MB samples and in the first heating scan for as spun fibers (FB-POY) and of drawn yarn (FB-FDY) (Fig. S1–S3 of Supplementary data). Examples of the DSC curves obtained during heating are shown in Fig. 1, in the case of blends with 20 wt.% PTT and pure components. After recording the first heating scan (curve b of Fig. 1), solution precipitated PET/PTT blends have been subjected to isothermal treatment for 5 min at 290 °C, prior cooling and recoding the II heating scans (curve b′ of Fig. 1). The melting temperature and enthalpy of SB samples are collected in Table 1 whereas those of MB and FB samples are shown in Table 2.

Regardless of preparation method, a single glass transition temperature (T_g) is observed (Table 1 and Fig. S1–S3), whose value gradually decreases with increase of PTT content from ≈80 °C for neat PET to ≈50 °C for neat PTT. The values of T_g for the various systems are reported in Fig. 2 as a function of composition. It is apparent that the glass transition temperature depends almost linearly on the composition of the mixtures [10,19], regardless of the preparation method of the sample. Only in the case of drawn yarns (FDY fibers) the T_g values are higher than those of other samples with the same PTT content, especially for neat PTT. The fact that the T_g values of FDY samples is higher than those of other samples is due to the effect of drawing at high temperatures that produces a decrease of mobility of chain in the amorphous regions due to occurrence of stress-induced (or enhancement of) crystallization and increase of degree of orientation of the chains in the crystalline and amorphous phases [20]. According to Supaphol

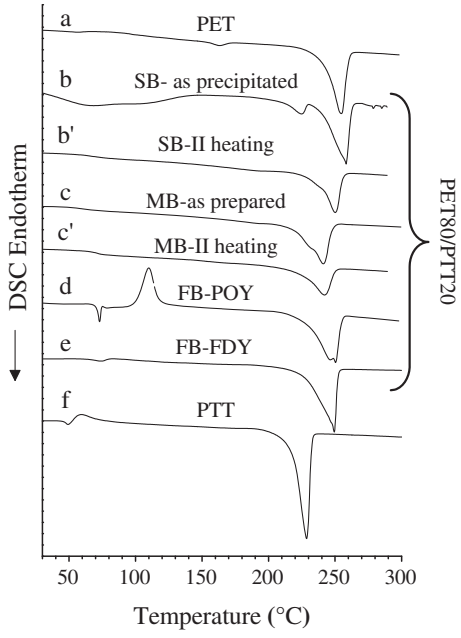

Fig. 1. DSC curves of PET (a), PTT (f) and PET/PTT blends with 20 wt.% PTT obtained by precipitation from solution (SB) (b, b′), melt extrusion (MB) (c, c′) and direct spinning of mechanical mixtures of neat components (d,e), in the case of as spun fibers (FB-POY, d) and drawn yarns (FB-FDY, e). a–f: First heating; b′, c′: Second heating. For SB sample after first heating scan, the melt has been kept for 5 min at 290 °C before cooling to room temperature and successive recording of II heating scan b.

Table 1
Glass transition temperature (T_g), melting temperature (T_m), and melting enthalpy (ΔH_m) of PET, PTT and PET/PTT blends obtained by precipitation from solution.[a]

PET wt.%/PTT wt.%	First heating scan							II heating scan (after 5 min at 290 °C and successive cooling)			
	T_g (°C)	T_{mPTT} (°C)	T_{mPET} (°C)	ΔH_{mPTT} (J/g)	$[\Delta H_{mPTT}]_c$(J/g)[b]	ΔH_{mPET}(J/g)	$[\Delta H_{mPET}]_c$ (J/g)[b]	T_g (°C)	T_m (°C)	ΔH_m (J/g)	$[\Delta H_m]_c$ (J/g)[c]
100/0	79.31	–	257.43	–	–	43.16	43.16	78.03	256.5	44.1	44.1
95/5	77.14	226.83	257.37	3.16	3.0405	47.39	41.002	75.17	251.9	40.71	41.9
90/10	74.04	227.17	257.83	7.73	6.081	46.21	38.844	72.31	251.8	35.66	39.69
80/20	69.91	224.67	258.5	10.97	12.162	46.86	34.528	67.66	250.3	35.22	35.28
70/30	68.39	225.83	258.33	16.2	18.243	40.89	30.212	66.82	245.3	36.91	30.87
0/100	48.91	226.27	–	60.81	60.81	–	–	49.11	226	61.6	–

[a] From DSC thermograms recorded at 10 °C/min of Figure S1.
[b] Calculated by multiplication of experimental ΔH_m values of neat components in the I heating scan (60.81 J/g for PTT and 43.16 J/g for PET) to the corresponding weight fraction.
[c] Calculated as $(\Delta H_m)_{PET}\, w_{PET}$ with $(\Delta H_m)_{PET} = 44.1$ J/g of PET in the second heating scan and w_{PET} the corresponding weight fraction.

et al., the presence of a single T_g in these systems is the hallmark that PET and PTT are miscible in the amorphous phase at segmental level [10].

The melting endotherms of as precipitated SB blends during the first heating scan (curve b of Fig. 1 and Fig. S1A) show, regardless of blend composition, two well separated peaks, located at temperatures of ≈226 and ≈257 °C corresponding to the melting temperature of pure PTT and PET, respectively. This indicates that the two components in the blends crystallize independent of each other upon precipitation from solution without formation of co-crystals. However, after melting and 5 min isotherm at 290 °C, a single broad crystallization peak occurs during the successive cooling scan (Fig. S1B), and the so formed crystals show a broad endotherm during the second heating scan (curve b′ of Fig. 1, and Fig. S1C) peaked at temperatures which gradually decrease with increasing PTT content in the blends. At variance with SB samples, MB samples show a single broad melting endotherm already during the first heating scan (curve c of Fig. 1 and Fig. S2A) at values close to those recorded during the second heating scan (curve c′ of Fig. 1 Fig. S2C). Also FB samples show a single broad melting peak (curves d,e of Fig. 1 and Fig. S3), independent of drawing treatment, the most remarkable difference being the fact that whereas as spun fibers (POY) crystallize during the DSC scan as indicated by the presence of an exothermal peak due to cold crystallization in the thermograms of Fig. 1 (curve d), drawn yarns (FDY) already fully crystallized during the hot drawing process and, hence, no cold crystallization occurs (curve e of Fig. 1, see also Fig. S3).

The melting temperatures of PET, PTT and PET/PTT samples obtained according to the different preparation methods are compared in Fig. 2B.

With the exception of as precipitated SB blends, melting point depression is clearly observed for all blends. The presence of a single melting peak instead of two and the large melting point depression with increasing the PTT concentration in melt processed PET/PTT blends may be attributed either to the occurrence of ester exchange reactions between the two components in the melt, leading to formation of copolymers [10–12] (see Scheme 1) or to thermodynamic effects, due to the lowered chemical potentials of the chains in the blends as compared to those of neat polyesters (thermodynamic effect), coupled to the smaller lamellar thickness achieved by crystals in presence of a second component (morphological effect) [21]. In particular, melting point depression of PET rich blends with PTT has been explained by Liang et al. [22] in the hypothesis of full miscibility of the two components in the melt, completely neglecting the eventual presence of copolymers formed in situ via ester exchange reactions during the melt processing of the initial mixture of the two components. Accordingly, the thermodynamic melting temperatures of PET in blends of different composition have been derived and, using the method by

Table 2
Glass transition temperature (T_g), melting temperature (T_m), and melting enthalpy (ΔH_m) of PET, PTT and PET/PTT blends obtained by melt extrusion in the first and second heating scans (MB) and of fibers obtained by melt spinning (FB) in the first heating scan.[a] The temperature (T_{cc}) and enthalpy (ΔH_{cc}) of cold crystallization of as spun fibers is also included.

PET wt.%/PTT wt.%	MB-I heating scan				MB-II heating scan			
	T_g (°C)	T_m (°C)	ΔH_m (J/g)	$[\Delta H_m]_{PET}$ (J/g)[b]	T_g (°C)	T_m (°C)	ΔH_m (J/g)	$[\Delta H_m]_{PET}$ (J/g)[b]
100/0	77.62	254.32	44.21	44.21	76.39	252.5	44.66	44.66
95/5	76.42	246	48.77	41.9995	75.91	249.7	47.61	42.427
90/10	73.36	240.38	45.99	39.789	73.11	248.2	46.17	40.194
80/20	70.99	243.71	46.07	35.368	70.62	242	47.11	35.728
70/30	67.88	208.36	35.67	30.947	66.97	233.7	36.19	31.262
0/100	45.81	226.67	61.5	–	46.03	224.6	58.14	–

PET wt.%/PTT wt.%	FB-POY[c]						FB-FDY[d]			
	T_g (°C)	T_{cc} (°C)	ΔH_{cc}(J/g)	T_m (°C)	ΔH_m(J/g)	$[\Delta H_m]_{PET}$ (J/g)[b]	T_g (°C)	T_m (°C)	ΔH_m(J/g)	$[\Delta H_m]_{PET}$ (J/g)[b]
100/0	76.17	107.5	22.24	258	42.46	42.46	80.17	253.67	57	57
95/5	75.5	108.17	26.32	257.17	48.74	40.34	79.17	254	55.59	54.15
90/10	75	110	20.75	250.83	46.02	38.21	78.17	251.83	54.41	51.3
80/20	73	108.5	25.55	250.5	46.17	33.97	74.33	249.67	49.84	45.6
70/30	70.5	109.5	22.62	245.17	35.75	29.72	80.17	243.5	40.57	39.9
0/100	44.3	58.3	6.36	225.9	60.97	–	79.17	223.83	67.16	–

[a] From DSC thermograms recorded at 10 °C/min.
[b] Calculated by multiplication of experimental ΔH_m values of neat PET to the PET weight fraction.
[c] Partially oriented yarns obtained at melt spinning speed of 3500 m/min.
[d] Fully drawn yarns obtained by drawing the corresponding POY samples.

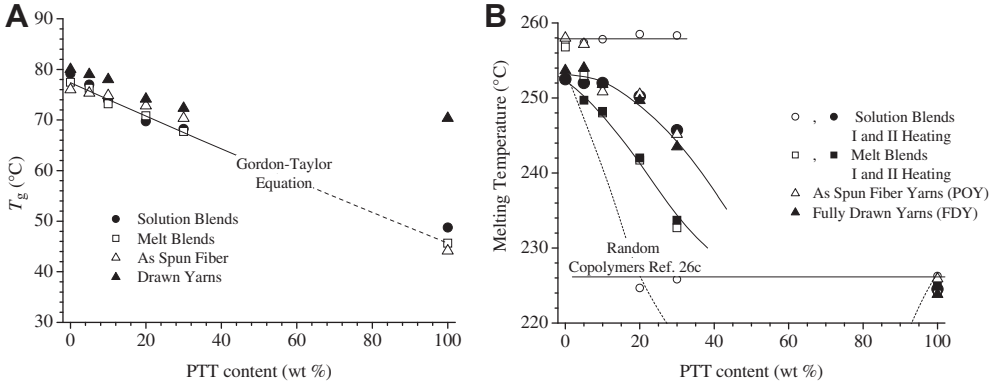

Fig. 2. A: Glass transition temperatures of PET and PTT and PET/PTT blends as a function of PTT content. The straight line is the fit to the data with the Gordon–Taylor equation with $K \approx 1$ (see ref. 10 and 20). B: Melting temperatures of PET and PTT and PET/PTT blends as a function of PTT content. SB samples obtained by precipitation from solution (○, ●), MB samples obtained by melt extrusion (□, ■), FB fibers obtained by direct spinning for as spun fibers (POY, △) and drawn yarns (FDY, ▲), and random copolymers of ref. 26c (dashed line). Melting temperatures of first heating scan (○, □) and second heating scan (●, ■).

Nishi and Wang [23], a negative value of ≈-0.16 for the χ interaction parameter has been obtained [22].

In our case, occurrence of ester exchange reactions with consequent formation of copolymers may not be neglected. Direct evidence of occurrence of these reactions has been obtained resorting to solution ^{13}C NMR spectroscopy, exploiting the high sensitivity of the chemical shift of quaternary aromatic carbons of terephthalate units (arrowed in Scheme 1) to the chemical environment [24]. As shown in Fig. 3 in the case of 70/30 PET/PTT blends, whereas as precipitated SB samples (curve a) show only two resonances at 133.5 and 133.7 ppm characteristic of PET and PTT neat components (carbons ET and TT of Scheme 1) in the case of SB samples crystallized from the melt after 5 min isotherm at 290 °C (curve b), and MB blends (curve c), extra peaks at 133.4 and 133.8 are also present due to the quaternary aromatic carbon atoms of terephthalate units in the mixed triad sequences -$O(CH_2)_2OCO$-(C_6H_4)-$OCO(CH_2)_3$- of the copolymer chains formed as a result of ester exchange reactions between the two components occurring in the melt (carbons ET' and TT' of Scheme 1).

The ^{13}C NMR analysis of Fig. 3 indicates that the lowering of melting temperature in melt crystallized samples is largely due to occurrence of ester exchange reactions. Only when transesterification reactions are prevented or reduced to a minimum as for instance by mixing the two polyesters at low temperature for less than 5 min [25] or in solution, each component keeps its own ability to crystallize, so that independent melting of PET and PTT may be observed at nearly the same temperature as the pure components. Formation of copolymers in the melt readily explains the remarkable decrease of melting temperature of PET with increase of concentration of minor component (Fig. 2B), and the fact that the exact values of melting temperature depends on the method of preparation of blends and/or the heat treatment in the melt state, which in turns, controls the extent to which transesterification reactions occur. In particular, the lower melting temperature of MB blends with respect to that of other systems indicate that under the conditions adopted for preparation of MB systems reactive blending leads to formation of copolymers with a distribution of units both inter- and intrachain more uniform than in the case of SB blends obtained from solution and successive melting in quiescent conditions (up to 290 °C), and of FB samples obtained by direct spinning. In the assumption that a more uniform distribution of units may be best approached by direct copolymerization of comonomers [26], in Fig. 2B the melting temperatures of our blends is compared with that of some poly(ethylene-*co*-trimethylene terephthalate) copolymers obtained in ref. 26c. It is apparent that the copolymers obtained by direct copolymerization of monomers exhibit lower melting temperatures than our blends and, for 1,3-propanediol content higher than 25 wt.%, these copolymers become unable to crystallize [26].

Occurrence of reactive blending upon melting with consequent formation of copolymers also explains the presence of a single crystallization exotherm of MB and SB blends in the DSC curves of Fig. S1B and S2B. The crystallization temperatures of MB and SB blends decrease with increasing PTT concentration and this decrease is parallel to the decrease of melting temperatures of SB

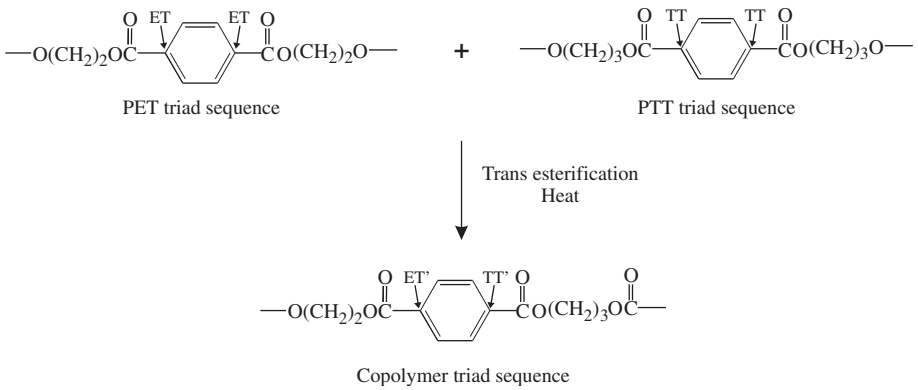

Scheme 1. Ester exchange reaction. Aromatic quaternary carbon atoms in different constitutional triad sequences are indicated.

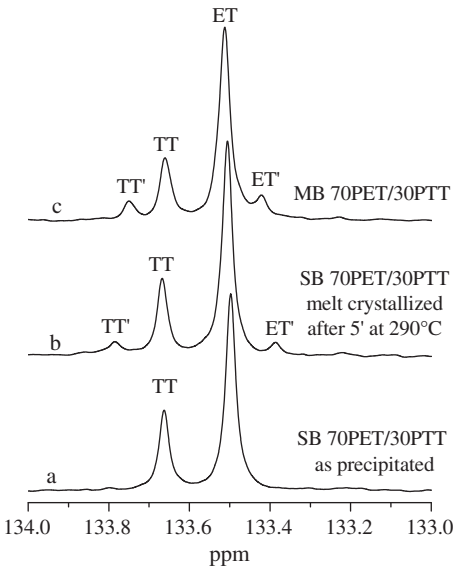

Fig. 3. Solution ^{13}C NMR spectra in the region of quaternary aromatic carbon atoms of indicated samples. The resonances characteristic of pure components (TT and ET) and of mixed triad sequences -O$(CH_2)_2$OCO-(C_6H_4)-OCO$(CH_2)_3$- of the copolymer chains formed as a result of ester exchange reactions (TT' and ET', see Scheme 1) are also indicated.

copolymers during the second heating (Fig. S1C) scan and of MB systems (Fig. S2C).

The results of the DSC analysis indicate that with the exception of as precipitated SB samples, in the case of blends obtained by melt extrusion, and direct spinning, as well as for the blends obtained by precipitation from solution after a heat treatment in the melt, the presence of single melting and crystallization peaks in the DSC thermograms is essentially due to the melting/crystallization of PET crystals. However, since the DSC peaks are broad, crystallization/melting from PTT segments may not be ruled out. In fact the crystallization/melting peak from PTT crystals may be easily buried by the broad exo/endothermal peak due to the crystallization/melting of the major component (PET).

3.2. X-ray diffraction analysis

In order to unravel the kind and the number of phases formed in our blends as a function of preparation method and/or thermal treatment, we have performed wide angle X-ray diffraction measurements.

The X-ray powder diffraction profiles of pure components and PET/PTT blends obtained by precipitation from solution and melt extrusion are shown in Fig. 4 (see also Fig. S4). In particular, the diffraction data of Fig. 4A are relative to as precipitated samples that have been melt pressed at 280 °C for less than 2 min and then cooled to room temperature by quenching in a water bath prior performing diffraction measurements. Examples of diffraction data collected for solution precipitated samples that have been crystallized from the melt at cooling rate of 10 °C/min in a DSC pan after isothermal treatment of the melt for 5 and 15 min at 290 °C are shown in Fig. 4B (curves a–c).

The crystal structure of PET has been studied by Daubeny and Bunn [27] years ago. The unit cell, which contains a single monomeric unit, is triclinic with parameters $a = 4.56$ Å $b = 5.94$ Å, $c = 10.75$ Å, $\alpha = 98.5°$, $\beta = 118°$, $\gamma = 112°$. PET chains adopt a nearly extended conformation in the crystals. Also PTT crystallizes in a triclinic unit cell, but with two monomeric units/cell. The unit cell

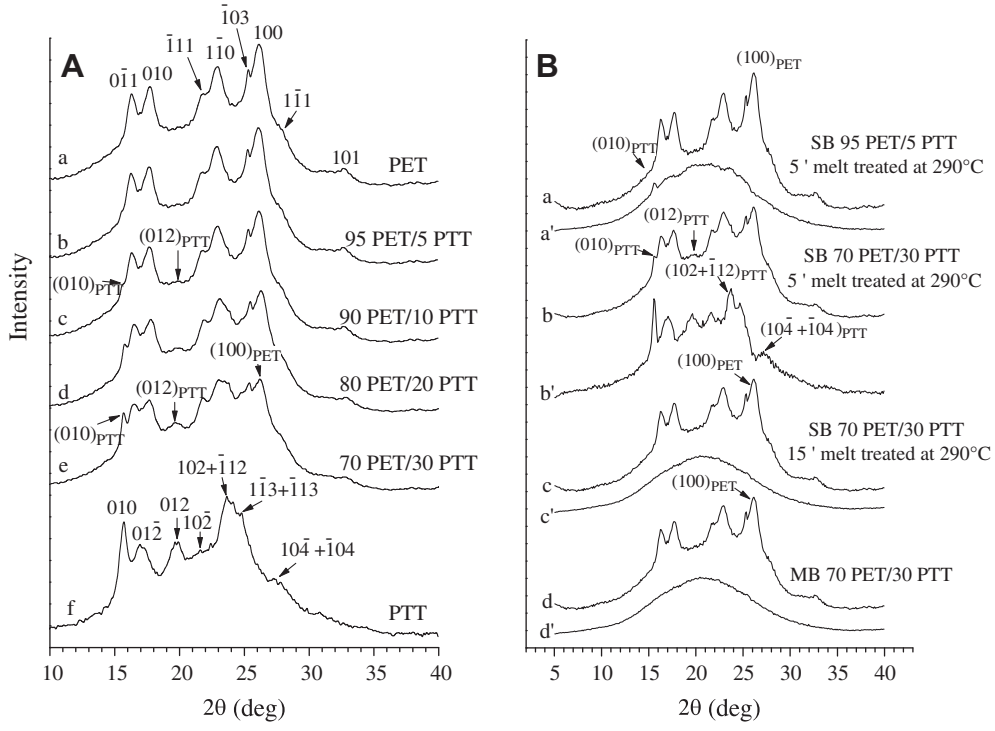

Fig. 4. X-ray powder diffraction profiles of (A) PET, PTT and PET/PTT blends obtained by precipitation from solution followed by compression molding at 280 °C for 2 min, and quenching in a water bath at room temperature, (B) PET95/PTT5 (a, a′) and PET70/PTT30 (b, b′, c,c′) blends obtained by precipitation from solution and then crystallized from the melt at 10 °C/min cooling rate after 5 min (a, a′,b,b′) and 15 min (c, c′) isotherm at 290 °C, and PET70/PTT30 blend obtained by melt extrusion (d,d′). In B, experimental diffraction profiles (a–d) and residual diffraction profiles (a′–d′). Curves a′–d′ are magnified by a factor inversely related to the mass fraction of PTT in the blend.

parameters of PTT change monotonically with increasing the macroscopic strain, and the exact values of unit cell parameters depend on the fiber draw ratio [28,29]. A good estimate of unit cell parameters recently performed on the basis of electron diffraction of single crystals and wide angle X-ray diffraction on powders and fibers is $a = 4.6$ Å $b = 6.1$ Å, $c = 18.6$ Å, $\alpha = 97.5°$, $\beta = 92.1°$, $\gamma = 110°$ [30]. The conformation of the chain in the crystals deviates from the fully trans-planar for the torsion angles around the two O-C—C-C bonds, which are both equal to $\approx +60°$ or $\approx -60°$ and in consecutive monomeric units alternate with opposite sign [29]. The large differences in the crystal structure of PET and PTT poses severe limitations to the possibility of forming co-crystals by crystallization of their mixtures. In Fig. 4A, for pure PET (curve a) the characteristic Bragg peaks of the triclinic form at $2\theta \approx 16.25$, 17.75, 21.85, 22.95, 25.35, 26.15, 27.65, and 32.65° are observed. They correspond to the reflections $0\bar{1}1$, 010, $\bar{1}11$, $1\bar{1}0$, $\bar{1}03$, 100, $1\bar{1}1$, and 101, respectively [27]. In the case of neat PTT, the X-ray diffraction profile shows Bragg peaks at $2\theta \approx 15.75$, 16.95, 19.65, 22.45, 23.65, 24.85, and 27.25° (curve f of Fig. 4A) corresponding to the reflections 010, $01\bar{2}$, 012, $10\bar{2}$, $102+\bar{1}12$, $1\bar{1}3+\bar{1}13$, and $10\bar{4}+\bar{1}14$, respectively, typical of the triclinic form of PTT [30].

In the diffraction profiles of as precipitated blends (curves b–e of Fig. 4A), the characteristic peaks of both PET and PTT are simultaneously present, in the same positions of pure PET and PTT, confirming that they consist of a mixture of crystals of the two components. It is possible identifying at least three reflections of PET and PTT which do not overlap, at $2\theta \approx 15.75$ and 19.65° for PTT and at $2\theta \approx 26°$ for PET. They correspond to $(010)_{PTT}$ and $(012)_{PTT}$ of PTT, and $(100)_{PET}$ of PET respectively.

Upon isothermal treatment of SB samples in the melt at 290 °C for 5 min, the $(010)_{PTT}$ and $(012)_{PTT}$ at $2\theta \approx 15.75$ and 19.65° of PTT become less discernible in the X-ray profiles of blends (curves a–b of Fig. 4B and S4B), and only the diffraction peaks of PET are clearly apparent. The presence of PTT crystals may be evidenced by subtraction from experimental profiles of the contribution from neat PET after scaling the corresponding diffraction profile for the mass fraction of PET in the blend. The corresponding residual diffraction profile shows Bragg peaks in the same positions as pure PTT (curves a′-b′ of Fig. 4B and S4B'). This indicates that after 5 min isotherm at 290 °C these samples still crystallize as mixtures of PET and PTT crystals, even though the crystallization ability of PTT is largely reduced due to formation of copolymer chains via ester exchange reactions (curve b of Fig. 3).

With increasing the annealing time of the melt at 290 °C, PTT loses almost completely its own ability to crystallize. In fact, as shown in Fig. 4B in the case of 70/30 PET/PTT SB sample (see also Fig. S4C), after 15 min isotherm at 290 °C (curve c of Fig. 4B) the X-ray diffraction profiles show exclusively the Bragg reflections at the same position and with the same relative intensity as pure PET. The corresponding residual diffraction (curve c′ of Fig. 4B and S4C'), does not show Bragg reflections but only a halo corresponding to the contribution from amorphous phase, regardless of PTT concentration in the blends.

The diffraction profiles of MB samples display exclusively reflections of pure PET (Fig. S4D). This is shown as an example in the case of 70/30 PET/PTT MB sample (curve d of Fig. 4B). The diffraction profiles of MB samples, indeed, after subtraction for crystalline PET contribution, do not show any residual Bragg peak (curve b′ of Fig. 4B).

Examples of X-ray fiber diffraction patterns of fiber yarns obtained by melt spinning of pure PET, pure PTT and PET/PTT blends are shown in Fig. 5. Since the X-ray diffraction patterns of blends are almost all identical, as an example, only the diffraction patterns of PET/PTT FB yarns with 30 wt.% PTT are shown in the Fig. 5B and B′.

In the case of POY, pure PET and PET/PTT blends (Fig. 5A, B) show a strong halo polarized on the equator and weak reflections (indicated with an arrow) polarized on the meridian at $2\sin\theta/\lambda \approx 0.29$

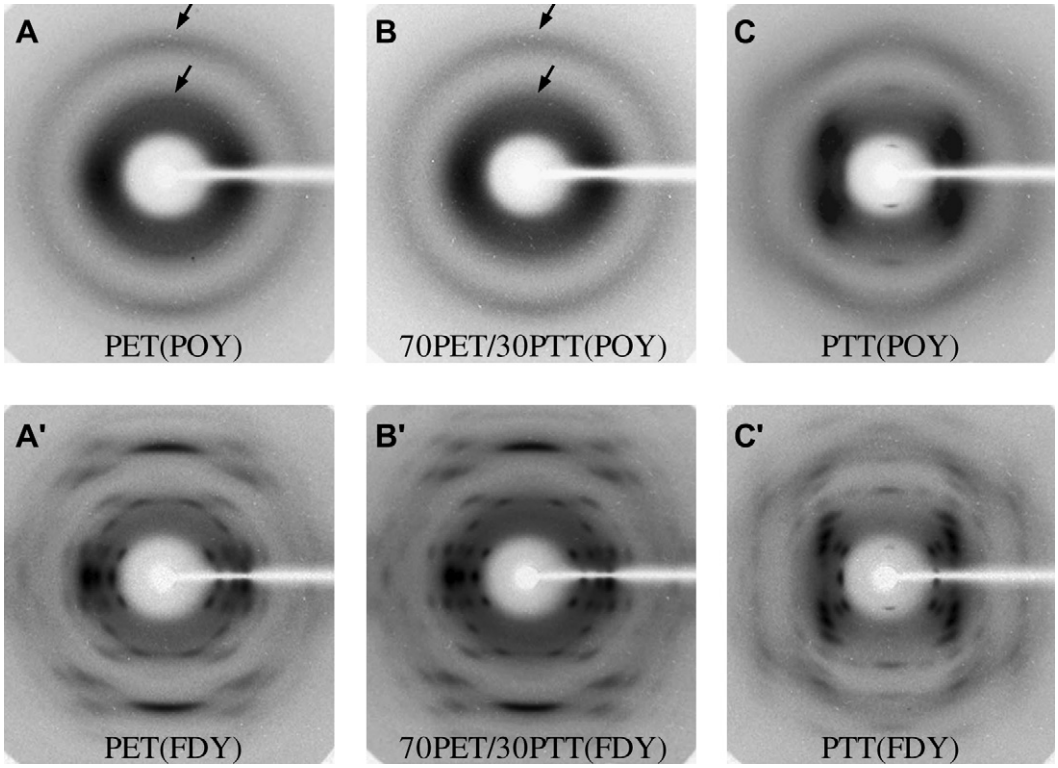

Fig. 5. X-ray fiber diffraction patterns of fiber yarns obtained by melt spinning of PET, PTT and PET/PTT blends with PTT concentration of 30 wt.%. A, B, C: as spun yarns (POY); A′, B′, C′; Drawn yarns (FDY). The meridional reflections at $2\sin\theta/\lambda \approx 0.29$ and 0.48 $Å^{-1}$ of mesomorphic form of PET are indicated with an arrow in A,B.

and 0.48 $Å^{-1}$ corresponding to the 3rd and 5-th order Bragg peaks of PET in the mesomorphic form, respectively, for a chain periodicity of 10.3 Å [31]. Pure PTT instead (Fig. 5C) shows broad diffraction peaks in the typical positions of the triclinic crystal structure [29]. This indicates that at spinning speed of 3500 m/min adopted for obtainment of POY samples PET is unable to crystallize, and only the mesomorphic form is obtained [31]. On the contrary, PTT, which shows a higher crystallization rate than PET, is more prone to crystallize, even though the crystals which are formed have small dimensions.

FDY samples show the typical diffraction patterns of well oriented and well crystallized fibers in the corresponding triclinic forms for pure PET (Fig. 5A′) [27], and pure PTT (Fig. 5C′) [28]. In the case of blends (Fig. 5B′), the X-ray fiber diffraction patterns of drawn FB samples (FDY) show Bragg peaks in the same positions and with same relative intensity as pure PET in the triclinic form. The absence of reflections of PTT confirms that also blends obtained by direct melt spinning consist of PET crystals intermingled with an amorphous phase where PTT segments are almost totally rejected and mixed with amorphous PET. Therefore, also in this case, the endothermic peak observed in the DSC curves of FB samples (Fig. 2) may be essentially ascribed to the melting of PET crystals Table 2.

The results of the present analysis indicate that in the case of blends obtained by melt extrusion and fiber blends as well as for the blends obtained by precipitation from solution after a heat treatment in the melt, the ability of PTT segments to crystallize is largely reduced. This may be due either to the too short length of PTT segments in the copolymers formed in situ via ester exchange reaction and/or to kinetic factors. The glass transition of the blends, indeed, is lower than that of PET but higher than that of PTT (Fig. 2A). This may easily increase the crystallization rate of PET sequences and decrease that of PTT segments. Since in the explored composition range PET is the majority component, the crystallization of the longer PET sequences overwhelms that of PTT sequences, reducing the mobility of the chains to the point that PTT segments remain frozen into the amorphous regions.

3.3. Effect of residence time of the melt at high temperatures

Since reactive blending occurs in the melt even in quiescent conditions, the effect of the residence time of the melt at high temperatures on the crystallization behavior of PET/PTT blends has been explored in the case of SB blends, recording DSC heating scans of the samples crystallized from the melt after isothermal treatment at 290 °C for different amounts of time (Fig. S5). Examples of DSC melting thermograms are shown in Fig. 6A in the case of SB PET80/PTT20 sample. The values of melting temperatures achieved by these blends upon increasing the residence time at 290 °C are shown in Fig. 6B (see also Table S1).

For pure components, the heat treatment of the melt at 290 °C has only a small effect on the melting temperature. In particular, the melting temperature of PET remains constant, whereas for pure PTT only a slight decrease occurs (Fig. 6B). The melting temperature of the blends, instead, decreases with respect to the value of neat PET by several degrees already for short residence time up to reach a nearly plateau value after ≈40 min (Fig. 6B). The temperature of the plateau depends on the blend composition, and decreases with increasing PTT concentration from ≈245 °C for the blend with 5 wt.% PTT, to ≈220 °C for the blend with 30 wt.% PTT (Fig. 6B). The glass transition temperature instead, is not greatly influenced by the residence time of the melt at 290 °C (Fig. S5 and Table S1).

3.4. Degree of crystallinity

The correct attribution of melting peaks in the DSC thermograms of blends to PET and/or PTT component achieved by diffraction analysis, allows for a confident evaluation of the degree of crystallinity of our blends, without ambiguity. In particular for as precipitated SB samples, which consist of mixtures of PET and PTT crystals melting independently one another at two different temperatures, the degree of crystallinity of PTT and PET components has been evaluated separately. For the remaining blends, the degree of crystallinity has been evaluated in the assumption that the melting enthalpy is exclusively due to the fusion of PET crystals, since the contribution from PTT is negligible or zero.

The degree of crystallinity of blends is reported in Fig. 7. It is apparent that the degree of crystallinity decreases only slightly by blending with respect to that of pure PET in the case of FB-POY and SB samples crystallized from the melt after isothermal treatment at 290 °C for more than 15 min. In the case of MB blends, FB-POY and for as precipitated SB systems, instead, the crystallinity of blends with PET content less than 20 wt.% is even higher than that of pure PET samples obtained with the same preparation procedure.

This indicates that whereas the formation of copolymers via ester exchange reactions between the two components in the blends decreases the crystallization ability of PTT, it does not influences the crystallization ability of PET segments. For short reaction times, reactive blending is incomplete, and only mixtures of PET and copolymers with long PET sequences covalently linked to short PTT segments are formed. For these mixtures a non negligible increment of crystallization ability of PET sequences is induced. With increasing the reaction time, the distribution of co-monomeric units both inter- and intra-chains becomes more

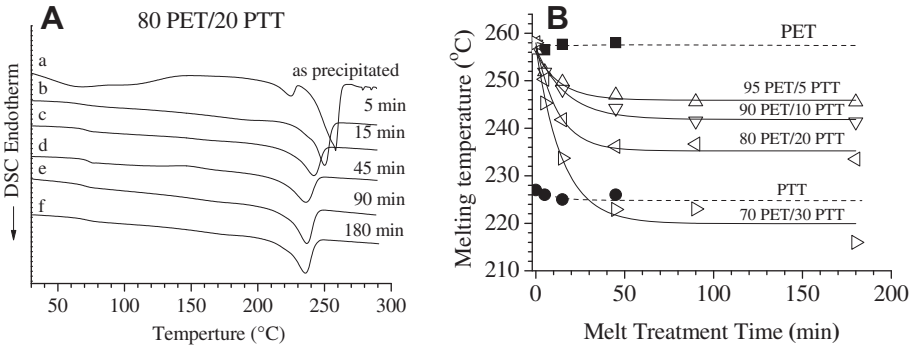

Fig. 6. (A): DSC melting endotherms of PET80/PTT20 mixtures obtained by precipitation from solution in the case of as precipitated samples (a) and of blends crystallized from the melt after keeping the melt at 290 °C for the indicated time (b–f). (B) Melting temperature of PET, PTT and PET/PTT blends obtained by precipitation from solution and successive crystallization from the melt after isothermal treatment at 290 °C for different amounts of time.

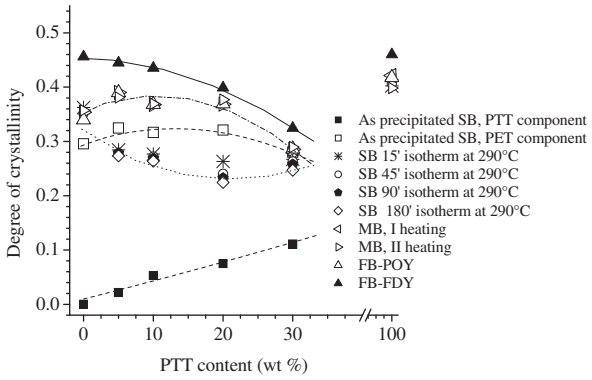

Fig. 7. Degree of crystallinity of PET in PET/PTT blends evaluated from DSC analysis. As precipitated solution blends, (□, ■); solution blends crystallized from melt after isothermal treatment at 290 °C for 15 (✳), 45 (○), 90 (⬟) and 180 (◇) min annealing at 290 °C; MB blends, first heating (◁) and II heating scan (▷); and FB-POY (△) and FB-FDY (▲) blends.

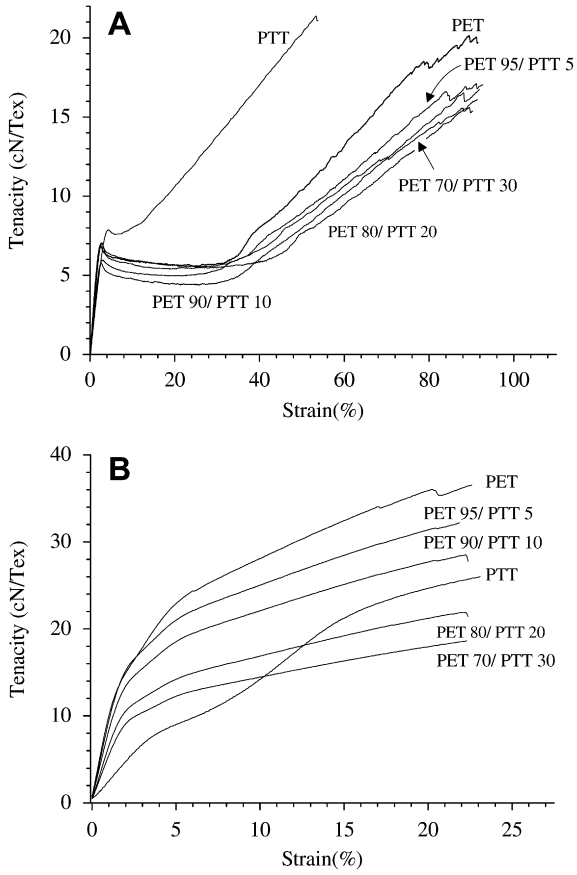

Fig. 8. Tenacity-strain curves of PET, PTT and PET/PTT blends obtained by melt spinning, (A) as spun fiber yarns (POY) and (B) drawn yarns. Curves are for aged samples. Tenacity is expressed as the ratio of applied load and the linear density of yarns.

and more uniform, and also the crystallization ability of PET segments tends to decrease.

The data of Fig. 7 suggest that by blending PET with PTT, PET rich blends may be obtained with the potential to give rise to a range of novel materials with chain microstructure and properties not only related to the composition of the blends, but also to the conditions of preparation and/or thermal history of the samples. These materials are characterized by glass transition temperatures intermediate between those of PET and PTT, whose precise values essentially depend on the composition of the blends. The melting temperature instead may be varied in a wide range for each composition, while preserving or even enhancing the crystallization ability of PET, just through changing the conditions of preparation of the blends (maximum temperature of the melt, crystallization from sheared melt, extrusion temperature, residence of the melt at high temperature).

3.5. Mechanical properties

The performance of this class of new materials is tested in the case of FB samples by measurements of mechanical properties. The tenacity-strain curves of PET, PTT and PET/PTT blends obtained by melt spinning are shown in Fig. 8. Data are shown for ≈1 year aged samples. The values of initial modulus, breaking tenacity and strain at breaking of fresh and aged samples are compared in Fig. 9 and Table S2.

For POY fibers (Fig. 8A), after the linear region of tenacity-strain curve and yield, a plateau region occurs, followed by a steep linear increase of tenacity up to break (strain hardening). For PTT-POY the plateau region is shorter than that of other samples, whereas, after the first linear region, higher values of tenacity at any strain are achieved up to breaking. Breaking occurs at 50–60% deformation values, which are lower than those achieved by PET, and PET/PTT blends POY samples prepared in similar conditions, which break at 90–100% deformation (Fig. 9C). The deformation behavior of PET and PET/PTT blends in POY samples is similar (Fig. 8A), with values of initial modulus (Fig. 9A) and breaking tenacity (Fig. 9B) gradually decreasing with increasing the PTT content, and similar values of elongation at break (Fig. 9C), regardless of aging time. The mechanical behavior of POY fibers of Fig. 8A reflects the results of structural analysis (Fig. 5), indicating that the melt spinning process at 3500 m/min produces fiber yarns in the mesomorphic form of PET in the case of PET and PET/PTT blends, whereas small crystals in the triclinic form are formed in the case PTT. The formation of mesophase instead of crystals in as spun fibers, both for PET and PET-rich blends, indeed, explains the lower tensile strength and tenacity values at any strain (Fig. 8A) experienced by these samples with respect to the crystalline POY fiber yarns.

The mechanical behavior of fully drawn yarns (FDY) (Fig. 8B) is markedly different from that of POY samples (Fig. 8A). The hot drawing of POY samples, in fact, produces fibers containing well formed crystals with a high degree of orientation parallel to the fiber axis (Fig. 5), so that fibers with higher mechanical strength, higher initial modulus (Fig. 9A), higher tenacity at break (Fig. 9B) but lower deformation at break (Fig. 9C) than POY are obtained.

Within the FDY series, the tenacity-strain behavior of PET/PTT blends is similar to that of PET and markedly different from that of PTT drawn yarns. Drawn yarns of PET and PET rich blends show stress-strain behavior typical of oriented fibers from semi-crystalline thermoplastic materials, with a monotonic behavior up to failure (Fig. 8B), characterized by an initial linear increase of tenacity with deformation, followed by a second linear region which is less steep than the former, separated by no defined yielding. The values of tenacity at any strain for the blends decrease with increasing the PTT concentration. Moreover, with increasing the PTT concentration, a gradual decrease of the initial modulus (Fig. 9A) and tenacity at break (Fig. 9B) occurs, while the deformation at break is maintained constant to the value of ≈25% (Fig. 9C). These trends are quite expected on the basis of structural analysis (Fig. 5) indicating that in FB- FDY samples only the PET

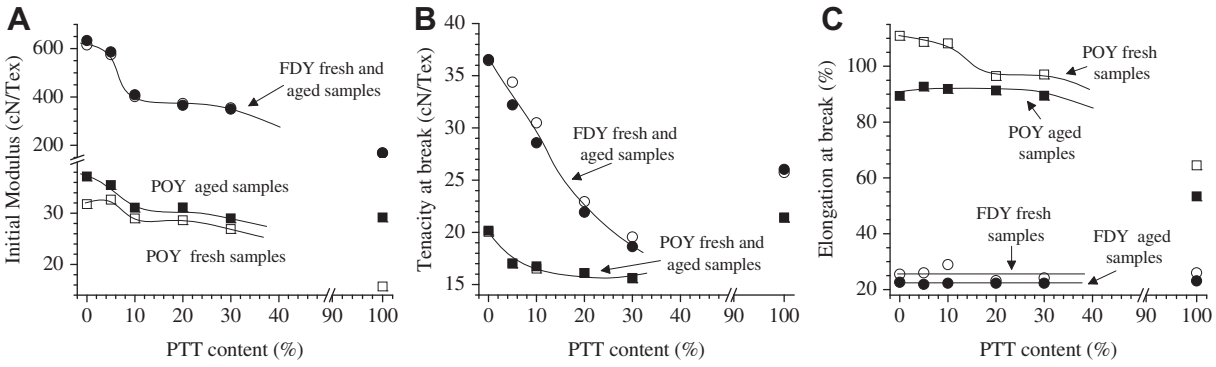

Fig. 9. (A) Initial modulus, (B) Tenacity at break and (C) Elongation at break of PET, PTT and PET/PTT blends obtained by melt spinning, for as spun fiber yarns (POY □, ■) and drawn yarns (FDY ○, ●) in the fresh state (□, ○) and after ≈ 1 year aging (■, ●).

component is able to crystallize. The gradual decrease of modulus with PTT concentration (Fig. 9A), in fact, is in agreement with the gradual decrease of crystallinity in FB blends (Fig. 7), whereas the behavior of blends at large deformations reflects the presence in the amorphous regions of PTT segments characterized by higher intrinsic flexibility than PET sequences.

The major differences, instead, reside in the shape of the tenacity-strain curves of FDY samples from PET and PET/PTT blends with respect to that of FDY sample from PTT (Fig. 8B). Drawn yarns of PTT, indeed, show a quite unconventional shape with a rather low values of initial modulus (Fig. 9A) and two characteristic yields at around 4 and 14% deformation separated by a nearly plateau region in the range 4–9% deformation (Fig. 8B). As already discussed in the literature [28,32], the unconventional shape of stress-strain curves of oriented fibers of PTT are due to the high deformability of PTT crystals in the direction parallel to the chain axis. PTT crystals, indeed, experience nearly affine deformation parallel to the *c*-axis up to 13–14% strain. For strains lower than 13–14%, deformations are largely reversible, and the fibers behave elastically. At strain higher than the 13–14%, however, close to the second yielding, plastic deformations also occur associated with irreversible movement of the chains both in the amorphous and crystalline regions. The high deformability of PTT crystals in the direction of chain axes are related to the fact that the conformation of the chains in the crystals deviate from the fully trans-planar because the torsion angles around the O-C—C-C bonds are both in the gauche state, resulting in a fiber identity period 76% of the repeat distance for a fully extended chain, consecutive monomeric units being inclined to the chain axis by ≈60°. It has been argued that the chains in the PTT crystals behave as coiled springs responding elastically to applied load for a rather large range of deformation (up to 13–14%) since O-C—C-C bonds may deviate from the gauche state quite easily. The pleated conformation of PTT chains in the crystals not only explains the peculiar shape of stress-strain curve of oriented fibers but also the fact that the initial modulus of drawn yarns from PTT is significantly lower than that of PET and PET/PTT yarns drawn in the same conditions (Fig. 9A). In PET crystals in fact, the chain axis conformation is close to the fully extended one, so that for highly oriented crystalline fibers, crystals respond to the stress with the usual deformation of bond lengths and valence angles. In the case of PTT, instead, changes of bond rotational angles should also occur [33].

4. Conclusions

The thermal behavior and the crystal structure of PET/PTT blends with PTT concentration lower than 30 wt.% prepared according to different methods have been comparatively studied. Direct relationships between the method of preparation of the blends, thermal and mechanical history of the samples, their structure, thermal and physical properties have been established.

PET and PTT are miscible in the melt and amorphous state, but not in the crystals. All blends, indeed, show a single glass transition temperature gradually decreasing with increasing the PTT concentration, whose precise value is essentially determined by the composition of the mixtures. Other properties, instead, such as melting temperature, crystallization ability of the two components, and degree of crystallinity are significantly influenced also by the preparation method.

Whereas two individual independent melting peaks as well as characteristic crystalline X-ray peaks of both components have been observed for blends prepared by precipitation from solution, in blends obtained by melt extrusion or direct spinning of mechanical mixtures of the two components only PET is able to crystallize, PTT being rejected into the amorphous regions. Significant decrease of melting temperature occurs in blends obtained by melt processing procedures, essentially due to formation of copolymer chains via ester exchange reactions occurring during the preparation step. Starting from mixtures obtained by co-precipitation from solution, it is clearly demonstrated that for blends crystallized from the melt after isothermal treatment at 290 °C for different amounts of time, the melting temperature decreases quite steeply for short residence time, and more gradually for longer time.

We argue that the effect of preparation method on the melting behavior and the degree of crystallinity of PET/PTT blends reflects the extent to which transesterification reactions between the two components occurs during the melt processing. For short residence time of the melt at high temperature, ester exchange reactions produce only a small fraction of copolymer chains with non uniform distribution of comonomers. Since the majority of chains remains essentially of PET type, the lower glass transition of the mixture with respect to that of pure PET enhances the ability of long PET sequences to crystallize, producing a small increase of the degree of crystallinity and/or crystal perfection. However, for annealing time higher than a critical value (40 min) the composition of the chains becomes more and more uniform, so that the average length of PET crystallizable sequences decreases, and also the degree of crystallinity starts decreasing.

A novel class of engineering materials is identified whose glass transition temperature is essentially fixed by the mixture composition, whereas the melting temperatures, for a given PTT content, may be controlled by the processing conditions, exploiting the

tendency of the two components to give rise to ester exchange reactions in the melt state. The performance of this class of materials is demonstrated in the case of FB samples by measurements of mechanical properties. It is shown that reactive blending of PET/PTT mixtures occurring in situ during extrusion and successive spinning is a versatile route for obtainment of PET-based fibers with good mechanical properties, relatively high crystallinity, variable melting temperatures and glass transition temperatures lower than that of pure PET.

Therefore, the practical importance of ester exchange reactions between PET and PTT chains during the melt processing has been clearly demonstrated. On a qualitative ground, it is clear that in the course of transesterification reactions the initial mixture of the two components gradually transforms into more complex mixtures including block copolymers, multi-block copolymers and eventually random copolymers. This indicates that the methods classically used to extract thermodynamic information related to the crystallization properties of binary blends of semi-crystalline polymers should be used with some caution in the case of PET/PTT blends. In fact, to a correct data analysis, it should be taken into account the possibility that during the heating/cooling runs generally used to probe the crystallization properties of these systems, the initial binary mixture of the two components may easily transform into mixtures including also copolymer chains. How the processing parameters used for the preparation of the blends (e.g. maximum temperature of the melt, application of shear stress, extrusion temperature, residence time of the melt at high temperature) really affect the chain microstructure in terms of molecular weight distribution and block length distribution, is still unclear. Since the latter parameters have large influence on the structure, physical and mechanical properties of the blends, the fine understanding of the effect of processing conditions on the evolution of chain microstructure, would enable one not only for a correct extraction of thermodynamic and kinetic parameters related to the crystallization properties of these blends but also to better control the reactive blending of PET and PTT polyesters as a powerful method for production of modified polyesters and polyester-based composites with specified properties.

Acknowledgments

Mr. Majid Khoshdel is gratefully acknowledged for preparation of FDY samples. We thank Dr. Vincenzo Perino of CIMCF (Centro Interdipartimentale di Metodologie Chimico Fisiche) of the University of Naples for assisting in the ^{13}C NMR measurements.

Appendix. Supplementary material

Supplementary data associated with this article can be found, in the online version, at doi:10.1016/j.polymer.2010.07.011.

References

[1] Fakirov S, editor. Handbook of thermoplastic polyesters: homopolymers, copolymers, blends, and composites, vol. I.. Weinheim: Wiley-VCH Verlag GmbH; 2002.
[2] Scheirs J, Long TE, editors. Modern polyesters: chemistry and technology of polyesters and copolyesters. Hoboken: Wiley; 2003.
[3] Traub HL. Die. Angew Makromol Chem 1995;179:4055.
[4] Supaphol P, Apiwanthanakom N. J Polym Sci Part B Polym Phys 2004;42:4151.
[5] Apiwanthanakom N, Supaphol P, Nithitanakul M. Polym Test 2004;23:817.
[6] Xu Y, Ye SR, Bian J, Quiam JM. J Mater Sci 2004;39:5551.
[7] Chung WT, Yeh WJ, Hong PD. J Appl Polym Sci 2002;83:2426.
[8] Utracki LA. Commercial polymer blends. London: Cahpman & Hall; 1998.
[9] Kuo YH, Woo EM. Polym J 2003;35:236.
[10] Supaphol P, Dangseeyun N, Thanomkiat P, Nithitanakul M. J Polym Sci Part B Polym Phys 2004;42:676.
[11] Choi KR, Chung GS, Lim KY, Kim BC. Polym Mater Sci Eng 2001;84:503.
[12] Castellano M, Turturro A, Valenti B, Avagliano A, Costa G. Macromol Chem Phys 2006;207:242.
[13] Oppermann W, Hirt P, Fritz C. Chem Fiber Int 1999;49:33.
[14] Becker O, Simon GP, Rieckmann T, Forsythe JS, Rosu RF, Volker S. J Appl Polym Sci 2002;83:1556.
[15] (a) Zimmer AG. Test method chemical process, titanium in polyester or polyamide (spectrophotometery), WN-B010–7061; 1996. (b) Zimmer AG. Test method chemical process, diethyleneglycol (DEG) in polyethylene terphethalate by gas chromatography, WN-B010–9008; 1996. (c) Zimmer AG, Test method chemical process, carbonyl end groups in polyester by potentiometric titration, WN-B010–7013; 1996.
[16] (a) Aharoni SM. Makromol Chem 1978;179:1867–71;
(b) Chuan HH, Lin-Vien D, Sono U. Polymer 2001;42:7137–9.
[17] (a) Mark JE, editor. Polymer data handbook. New York: Oxford University Press; 1999;
(b) Pyda M, Wunderlich B. J Polym Sci Part B Polym Phys 2000;38:622.
[18] Hammersley AP. ESRF internal report, ESRF98HA01T, FIT2D V9.129 Reference Manual V3.1; 1998. Hammersley AP, Svensson SO, Hanfland M, Fitch AN, Häusermann D. High Press Res 1996;14:235–48.
[19] Gordon M, Taylor JS. J Appl Chem USSR 1952;2:493.
[20] Samuels RJ. Structured polymer properties. New York: Wiley; 1974.
[21] Mandelkern L. Crystallization of polymers, vol. I. New York: Cambridge University Press; 2002;
Scott RL. J Chem Phys 1949;17:279;
Flory PJ. Principles of polymer chemistry. New York: Cornell University Press; 1953.
[22] Liang H, Xie F, Chen B, Guo F, Jin Z, Luo F. J Appl Polym Sci 2008;107:431.
[23] Nishi T, Wang TT. Macromolecules 1975;8:909.
[24] Litmanovich AD, Platé NA, Kudryavtsev YV. Prog Polym Sci 2002;27:915;
Son TW, Kim KI, Kim NH, Jeong MG, Kim YH. Fibers Polym 2003;1:20;
Spera S, Po R, Abis L. Polymer 1996;37:729;
Backson SCE, Kenwright AM, Richards RW. Polymer 1995;36:1991.
[25] Run M, Hao Y, Yao C. Therm Acta 2009;495:51.
[26] (a) Zou H, Li G, Jiang J, Yang S. Polym Eng Sci 2008;48:511;
(b) Chen X, Yang K, Hou G, Chen Y, Dong Y, Liao Z. J Appl Polym Sci 2007;105:3069;
(c) Wu T-M, Lin Y-W. J Polym Sci Part B 2004;42:4255.
[27] Daubeny Rde P, Bunn CW. Proc R Soc Lond A 1954;226:531.
[28] Jakeways R, Ward IM, Wilding MA, Hall IH, Desborough IJ, Pass MG. J Polym Sci Part B 1975;13:799.
[29] Poulin-Dandurand S, Perez S, Revol J-F, Brisse G. Polymer 1979;20:419.
[30] Wang B, Li CY, Hanzlicek J, Cheng SZD, Geil P, Grebowicz J, et al. Polymer 2001;42:7171.
[31] Asano T, Seto T. Polym J 1973;5:72;
Hinrichsen G, Adam HG, Krebs H, Springer H. Colloid Polym Sci 1980;258:232;
Napolitano MJ, Moet A. J Appl Polym Sci 1987;34:1285;
Fakirov S, Evstatiev M. Polymer 1990;31:431;
Parravicini L, Leone B, Auriemma F, Guerra G, Petraccone V, Di Dino G, et al. J Appl Polym Sci 1994;52:875;
Auriemma F, Corradini P, De Rosa C, Guerra G, Petraccone V, Bianchi R, et al. Macromolecules 1992;25:2490.
[32] Chen K, Tang X. J Appl Polym Sci 2004;91:1967.
[33] Ward IM, Wilding MA, Brody H. J Polym Sci Part B 1976;14:263.